

Constant Mean Curvature Surfaces with Two Ends in Hyperbolic Space

Wayne Rossman, Katsunori Sato

April 29, 2008

Abstract

We investigate the close relationship between minimal surfaces in Euclidean 3-space and constant mean curvature 1 surfaces in hyperbolic 3-space. Just as in the case of minimal surfaces in Euclidean 3-space, the only complete connected embedded constant mean curvature 1 surfaces with two ends in hyperbolic space are well-understood surfaces of revolution – the catenoid cousins.

In contrast to this, we show that, unlike the case of minimal surfaces in Euclidean 3-space, there do exist complete connected immersed constant mean curvature 1 surfaces with two ends in hyperbolic space that are not surfaces of revolution – the genus 1 catenoid cousins. The genus 1 catenoid cousins are of interest because they show that, although minimal surfaces in Euclidean 3-space and constant mean curvature 1 surfaces in hyperbolic 3-space are intimately related, there are essential differences between these two sets of surfaces. The proof we give of existence of the genus 1 catenoid cousins is a mathematically rigorous verification that the results of a computer experiment are sufficiently accurate to imply existence.

1 Introduction

The main result presented in this paper is motivated primarily by a result of Schoen [S], that the only complete connected finite-total-curvature minimal immersions in \mathbb{R}^3 with two embedded ends are catenoids. In this paper we investigate the closely related case of constant mean curvature (CMC) 1 surfaces with two ends in hyperbolic space \mathbb{H}^3 . Other motivations are the results of Kapouleas, Korevaar, Kusner, Meeks, and Solomon. In [KKS] it was shown that any complete properly embedded nonminimal CMC surface with two ends in \mathbb{R}^3 is a periodic surface of revolution (Delaunay surface). In [K] it was shown that there exist immersed complete nonminimal CMC surfaces with two ends in \mathbb{R}^3 with genus $g \geq 2$. And in [KKMS] it was shown that any complete properly embedded CMC c ($c > 1$) surface with two ends in \mathbb{H}^3 is a periodic surface of revolution (hyperbolic Delaunay surface).

CMC 1 surfaces in \mathbb{H}^3 are closely related to minimal surfaces in \mathbb{R}^3 . There is a natural correspondence between them, known as Lawson's correspondence. Let \mathcal{U} be a simply-connected region of \mathbb{C} . If $x : \mathcal{U} \rightarrow \mathbb{R}^3$ is a local representation for a minimal surface in \mathbb{R}^3 with first and second fundamental forms I and II , then we see (via the Gauss and Codazzi equations and the fundamental theorem for surfaces) that there is a well-defined CMC 1 surface $\tilde{x} : \mathcal{U} \subset \mathbb{C} \rightarrow \mathbb{H}^3$ with first and second fundamental forms I and $II + I$. In addition, CMC 1 surfaces in \mathbb{H}^3 have a Weierstrass representation based on a pair of holomorphic functions [B], similar to the Weierstrass representation for minimal surfaces in \mathbb{R}^3 (see section 2).

The following theorem was first proven by Levitt and Rosenberg, and holds for any CMC c surface, not just for surfaces satisfying $c = 1$. We include a proof here (section 3) for the sake of completeness.

Theorem 1.1 [LR] *Any complete properly embedded CMC c surface in \mathbb{H}^3 with asymptotic boundary consisting of at most two points is a surface of revolution. In particular, it is homeomorphic to a punctured sphere.*

In the case that $c = 1$, this theorem implies that the surface must be a genus 0 catenoid cousin. (This was shown in [UY1]. The genus 0 catenoid cousins were originally described in [B].) The condition that the surface has asymptotic boundary at most two points implies that $c \geq 1$, as shown by do Carmo, Gomes, and Thorbergsson [CGT].

We will show that the condition “embedded” is critical to the above theorem, by giving an immersed counterexample, which we call the genus 1 catenoid cousin.

Theorem 1.2 *There exists a one-parameter family of CMC 1 genus 1 complete properly immersed surfaces in \mathbb{H}^3 with asymptotic boundary consisting of two points.*

The genus 1 catenoid cousin demonstrates a clear difference between CMC 1 surfaces in \mathbb{H}^3 and minimal surfaces in \mathbb{R}^3 , since Schoen's result on minimal surfaces in \mathbb{R}^3 holds even for immersions.

The genus 1 catenoid cousin further shows that the set of CMC 1 surfaces in \mathbb{H}^3 with embedded ends is in some sense larger than the set of minimal surfaces in \mathbb{R}^3 with embedded ends. Loosely speaking, the set of complete minimal surfaces with embedded ends in \mathbb{R}^3 can be mapped injectively to a set of (one-parameter families of) corresponding complete CMC 1 surfaces with embedded ends in \mathbb{H}^3 ([RUY]). The second theorem above shows that we cannot map the set of (one-parameter families of) complete CMC 1 surfaces with embedded ends in \mathbb{H}^3 injectively to a set of corresponding complete minimal surfaces with embedded ends in \mathbb{R}^3 , since there does not exist a minimal surface in \mathbb{R}^3 which corresponds to the genus 1 catenoid cousin in \mathbb{H}^3 .

In section 4 we give a nonrigorous explanation for why one should expect the genus 1 catenoid cousins to exist. The remainder of the paper is then devoted to proving Theorem 1.2 rigorously. We believe that the proof has two interesting characteristics:

- One is that the period problems that must be solved can be reduced to a single period problem, using symmetry properties of the surface, by a fairly direct argument. This kind of dimension reduction of the period problem can usually be done in a geometric and uncomplicated way for minimal surfaces in \mathbb{R}^3 , but for CMC 1 surfaces in \mathbb{H}^3 this kind of dimension reduction seems to be inherently more algebraic and less geometrically transparent [RUY].
- The other is that we then solve the single remaining period numerically, and then we use a mathematically rigorous analysis of the numerical method to conclude that the numerical results are correct. Certainly, this kind of “numerical error analysis” has been used before, for example in [HHS] and [KPS], and it is likely to be used frequently in the future, as it is well suited for solving period problems on surfaces for which no other method of solution can be found. It is easy to imagine how this method could be useful in a very wide variety of situations.

We solve the single period problem by applying the intermediate value theorem. The idea is similar to the way the intermediate value theorem is used in the conjugate Plateau construction to solve period problems for minimal surfaces in \mathbb{R}^3 [Kar], [BR]. However, the conjugate Plateau construction fails to help us in the study of CMC 1 surfaces in \mathbb{H}^3 , hence we have used numerical analysis instead. (The conjugate Plateau construction *is* of use in studying *minimal* surfaces in \mathbb{H}^3 [P], but does not appear to be useful for studying CMC 1 surfaces in \mathbb{H}^3 .)

The same methods we use here could likely also be applied to produce similar examples with two ends and genus greater than one, without any conceptual additions. However, with genus greater than 1, after reducing the period problems to a minimal set, we would still have at least a 2-dimensional problem, and thus the computational aspects would become much more involved. As the genus 1 example fulfills our goal of finding a counterexample to Schoen’s result in the hyperbolic case (and is computationally more easily understandable), we felt it was appropriate to restrict ourselves to genus 1.

Although this paper is written from a mathematical viewpoint, the arguments used here became apparent to the authors only by means of a numerical experiment. Hence, from the authors’ point of view, experimental results were essential in obtaining the above result.

2 The Weierstrass representation

Both minimal surfaces in \mathbb{R}^3 and CMC 1 surfaces in \mathbb{H}^3 can be described parametrically by a pair of meromorphic functions on a Riemann surface, via a Weierstrass representation. First we describe the well-known Weierstrass representation for minimal surfaces in \mathbb{R}^3 . We will incorporate into this representation the fact that any complete minimal surface of finite total curvature is conformally equivalent to a Riemann surface Σ with a finite number of points $\{p_j\}_{j=1}^k \subset \Sigma$ removed ([O]):

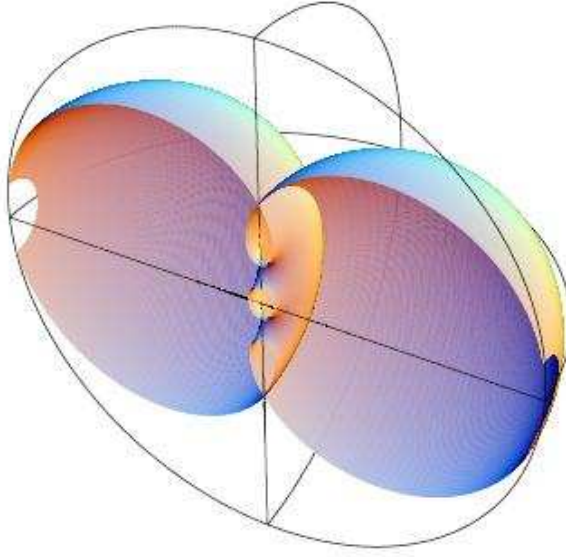


Figure 1: A genus 1 catenoid cousin in the Poincare model for \mathbb{H}^3 . (Half of the surface has been cut away.)

Lemma 2.1 *Let Σ be a Riemann surface. Let $\{p_j\}_{j=1}^k \subset \Sigma$ be a finite number of points, which will represent the ends of the minimal surface defined in this lemma. Let z_0 be a fixed point in $\Sigma \setminus \{p_j\}$. Let g be a meromorphic function from $\Sigma \setminus \{p_j\}$ to the complex plane \mathbb{C} . Let f be a holomorphic function from $\Sigma \setminus \{p_j\}$ to \mathbb{C} . Assume that, for any point in $\Sigma \setminus \{p_j\}$, f has a zero of order $2k$ at some point if and only if g has a pole of order k at that point, and assume that f has no other zeroes on $\Sigma \setminus \{p_j\}$. Then*

$$\Phi(z) = \operatorname{Re} \int_{z_0}^z \begin{pmatrix} (1 - g^2)fd\zeta \\ i(1 + g^2)fd\zeta \\ 2gfd\zeta \end{pmatrix}$$

is a conformal minimal immersion of the universal cover $\Sigma \setminus \{\widetilde{p_j}\}$ of $\Sigma \setminus \{p_j\}$ into \mathbb{R}^3 . Furthermore, any complete minimal surface in \mathbb{R}^3 can be represented in this way.

The map g can be geometrically interpreted as the stereographic projection of the Gauss map. The first and second fundamental forms and the intrinsic Gaussian curvature for the surface $\Phi(z)$ are

$$ds^2 = (1 + g\bar{g})^2 f\bar{f}dzd\bar{z}, \quad II = -2\operatorname{Re}(Q), \quad K = -4 \left(\frac{|g'|}{|f|(1 + |g|^2)^2} \right)^2,$$

where $Q = fg'dz^2$ is the Hopf differential.

To make a surface of finite total curvature $\int_{\Sigma} -KdA < +\infty$, we must choose f and g so that Φ is well defined on $\Sigma \setminus \{p_j\}$ itself. Usually this involves adjusting some

real parameters in the descriptions of f and g and $\Sigma \setminus \{p_j\}$ so that the real part of the above integral about any nontrivial loop in $\Sigma \setminus \{p_j\}$ is zero.

We now describe a Weierstrass type representation for CMC c surfaces in $\mathbb{H}^3(-c^2)$. ($\mathbb{H}^3(-c^2)$ is a simply-connected complete 3-dimensional space with constant sectional curvature $-c^2$. $\mathbb{H}^3 := \mathbb{H}^3(-1)$.) This lemma is a composition of results found in [B], [UY3], and [UY4].

Lemma 2.2 *Let Σ , $\Sigma \setminus \{p_j\}$, z_0 , f , and g be the same as in the previous lemma. Choose a null holomorphic immersion $F : \Sigma \setminus \{p_j\} \rightarrow SL(2, \mathbb{C})$ so that $F(z_0)$ is the identity matrix and so that F satisfies*

$$F^{-1}dF = c \begin{pmatrix} g & -g^2 \\ 1 & -g \end{pmatrix} f dz, \quad (2.1)$$

then $\Phi : \Sigma \setminus \{p_j\} \rightarrow \mathbb{H}^3(-c^2)$ defined by

$$\Phi = \frac{1}{c} F^{-1} \overline{F^{-1}}^t \quad (2.2)$$

is a conformal CMC c immersion into $\mathbb{H}^3(-c^2)$ with the Hermitean model. Furthermore, any CMC c surface in $\mathbb{H}^3(-c^2)$ can be represented in this way.

A description of the Hermitean model can be found in any of [B], [UY1], and [UY2], but we also briefly describe it here. If \mathcal{L}^4 denotes the standard Lorentzian 4-space of signature $(-+++)$, then the Minkowsky model for $\mathbb{H}^3(-c^2)$ is $\mathbb{H}^3(-c^2) = \{(t, x_1, x_2, x_3) \in \mathcal{L}^4 : \sum_{j=1}^3 x_j^2 - t^2 = \frac{-1}{c^2}\}$. We can identify each point (t, x_1, x_2, x_3) in the Minkowsky model with a point

$$\begin{pmatrix} t + x_3 & x_1 + ix_2 \\ x_1 - ix_2 & t - x_3 \end{pmatrix}$$

in the space of 2×2 Hermitean matrices. Thus the Hermitean model for $\mathbb{H}^3(-c^2)$ is

$$\mathbb{H}^3(-c^2) = \{\pm \frac{1}{c} a \cdot \bar{a}^t : a \in SL(2, \mathbb{C})\}.$$

We call g the *hyperbolic Gauss map* of Φ . As its name suggests, the map $g(z)$ has a geometric interpretation for this case as well. It is the image of the composition of two maps. The first map is from each point z on the surface to the point at the sphere at infinity in the Poincare model which is at the opposite end of the oriented perpendicular geodesic ray starting at z on the surface. The second map is stereographic projection of the sphere at infinity to the complex plane \mathbb{C} [B]. The first and second fundamental forms and the intrinsic Gaussian curvature of the surface are

$$ds^2 = (1 + G\bar{G})^2 \frac{fg'}{G'} \overline{\left(\frac{fg'}{G'}\right)} dz d\bar{z}, \quad II = -2\text{Re}(Q) + c ds^2, \quad K = -4 \left(\frac{|G'|^2}{|g'| |f| (1 + |G|^2)^2} \right)^2,$$

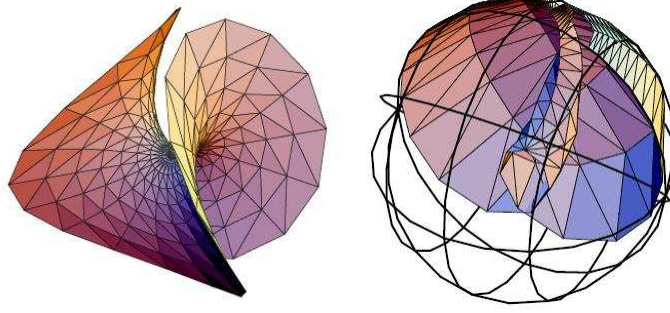


Figure 2: A minimal Enneper surface in \mathbb{R}^3 , and half of an Enneper cousin in the Poincare model for \mathbb{H}^3 . The entire Enneper cousin consists of the piece above and its reflection across the plane containing the planar geodesic boundary.

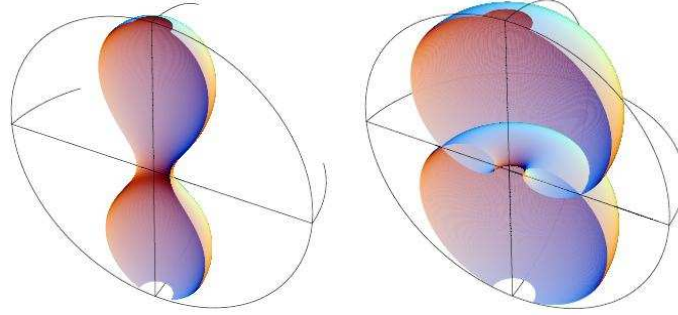


Figure 3: Two different genus 0 catenoid cousins in the Poincare model for \mathbb{H}^3 . The surface on the left is embedded, and the surface on the right is not embedded.

where in this case the Hopf differential is $Q = -fg'dz^2$ (the sign change in Q is due to the fact that we are considering the “dual” surface; see [UY4] for an explanation of this), and where G is defined as the multi-valued meromorphic function

$$G = \frac{dF_{11}}{dF_{21}} = \frac{dF_{12}}{dF_{22}}$$

on $\Sigma \setminus \{p_j\}$, with $F = (F_{ij})_{i,j=1,2}$. The reason that G is multi-valued is that F itself can be multi-valued on $\Sigma \setminus \{p_j\}$ (even if Φ is well defined on $\Sigma \setminus \{p_j\}$ itself). The function G is called the *secondary Gauss map* of Φ ([B]).

In the above lemma, we have changed the notation slightly from the notation used in [B], because we wish to use the same symbol “ g ” both for the map g for minimal surfaces in \mathbb{R}^3 and for the hyperbolic Gauss map for CMC c surfaces in $\mathbb{H}^3(-c^2)$. And we further wish to give a separate notation “ G ” for the secondary Gauss map used in the hyperbolic case. We do this to emphasize that the “ g ” in the Euclidean case is more closely related to the hyperbolic Gauss map “ g ” in the \mathbb{H}^3 case than to the geometric Gauss map “ G ”.

We now describe some simple examples:

- The horosphere is a CMC 1 surfaces in \mathbb{H}^3 . It has Weierstrass data $\Sigma \setminus \{p_j\} = \mathbb{C}$, $g = 1$, $f = 1$.
- The Enneper cousins ([RUY]) (see Figure 2) have Weierstrass data $\Sigma \setminus \{p_j\} = \mathbb{C}$, $g = z$, $f = \lambda \in \mathbb{R}$.
- The catenoid cousins ([B], [UY1]) (see Figure 3) have Weierstrass data $\Sigma \setminus \{p_j\} = \mathbb{C} \setminus \{0\}$, $g = z$, $f = \frac{\lambda}{z^2} \in \mathbb{R}$. These surfaces are either embedded or not embedded, depending on the value of λ .

We now state some known facts, which when taken together, further show just how closely related CMC 1 surfaces in \mathbb{H}^3 are to minimal surfaces in \mathbb{R}^3 .

- It was shown in [UY2] that if f and g and $\Sigma \setminus \{p_j\}$ are fixed, then as $c \rightarrow 0$, the CMC c surfaces Φ in $\mathbb{H}^3(-c^2)$ converge locally to a minimal surface in \mathbb{R}^3 . This can be intuited from the fact that $G \rightarrow g$ as $c \rightarrow 0$ (which follows directly from equation 2.1), and hence the above first and second fundamental forms for the CMC c surfaces Φ converge to the fundamental forms for a minimal surface as $c \rightarrow 0$ (up to a sign change in II – a change of orientation). The resulting minimal surface does not necessarily have the same global topology as the CMC c surfaces, and it may be periodic.
- Consider the Poincare model for $\mathbb{H}^3(-c^2)$ for $c \approx 0$. It is a round ball in \mathbb{R}^3 centered at the origin with Euclidean radius $\frac{1}{|c|}$ endowed with a complete radially-symmetric metric $ds_c^2 = \frac{4 \sum dx_i^2}{(1 - c^2 \sum x_i^2)^2}$ of constant sectional curvature $-c^2$. Contracting this model by a factor of $|c|$, we obtain a map to the Poincare model for \mathbb{H}^3 . Under this mapping, CMC c surfaces are mapped to CMC 1 surfaces. Thus the problem of existence of CMC c surfaces in $\mathbb{H}^3(-c^2)$ for $c \approx 0$ is equivalent to the problem of existence of CMC 1 surfaces in \mathbb{H}^3 .
- It was shown in [RUY] that a finite-total-curvature minimal surface in \mathbb{R}^3 satisfying certain conditions (these conditions are fairly general and include most known examples) can be deformed into a CMC c surface in $\mathbb{H}^3(-c^2)$ for $c \approx 0$, so that Σ , f , and g are the same, up to a slight adjustment of the real parameters that are used to solve the period problems. By the previous item, these surfaces are equivalent to CMC 1 surfaces in \mathbb{H}^3 , thus we have a 1-parameter family of CMC 1 surfaces in \mathbb{H}^3 with parameter c . The deformed surfaces might not have finite total curvature, but they will be of the same topological type as the minimal surface, and they will have the same reflectional symmetries as the minimal surface. (See Section 4.)

Regarding the last item above, Theorem 1.2 shows that the converse of the [RUY] result does not hold.

3 Embedded Case

The proof of Theorem 1.1 uses the maximum principle and Alexandrov reflection. Before stating the maximum principle, we define some terms. If Σ_1 and Σ_2 are two smooth oriented complete hypersurfaces of \mathbb{H}^n which are tangent at a point p and have the same oriented normal at p , we say that p is a *point of common tangency* for Σ_1 and Σ_2 . Let the common tangent geodesic hyperplane \mathcal{P} through p have the same orientation as Σ_1 and Σ_2 at p . Then, near p , expressing Σ_1 and Σ_2 as graphs $g_1(x)$ and $g_2(x)$ over points $x \in \mathcal{P}$ (the term *graph* in this context is defined in [CL]), we say that Σ_1 *lies above* Σ_2 near p if $g_1 \geq g_2$.

Proposition 3.1 (*Maximum Principle*) *Suppose that Σ_1 and Σ_2 are closed oriented hypersurfaces in \mathbb{H}^n with the same constant mean curvature c and the same smooth boundary $\partial\Sigma_1 = \partial\Sigma_2$. Suppose that Σ_1 and Σ_2 have a point p of common tangency, and that Σ_1 lies above Σ_2 near p . (The point p can be either an interior point of both Σ_1 and Σ_2 or a boundary point of both Σ_1 and Σ_2 .) Then $\Sigma_1 = \Sigma_2$.*

The above proposition is well known, and proofs can be found in [KKMS], [CL], and references therein.

In the Poincare model for \mathbb{H}^3 ($B^3 = \{x \in \mathbb{R}^3, |x| < 1\}$ with the metric $ds^2 = \frac{4|dx|^2}{(1-|x|^2)^2}$), the totally geodesic planes are the intersections of B^3 with spheres and planes in \mathbb{R}^3 which meet ∂B^3 orthogonally. We shall use the Poincare model and these totally geodesic planes in the proof of Theorem 1.1, which we now give.

Proof. We consider a complete properly embedded CMC surface M in \mathbb{H}^3 . First we suppose that M has asymptotic boundary consisting of exactly two points. Applying an isometry of \mathbb{H}^3 if necessary, we may assume that these two asymptotic points are at the north and south poles $(0, 0, \pm 1)$.

Let \vec{v} be a horizontal unit vector in \mathbb{R}^3 . For $t \in (-1, 1)$, let P_t be the totally geodesic plane containing the point $t\vec{v}$ and perpendicular to the line through \vec{v} . The plane P_t separates \mathbb{H}^3 into two regions: let A_t be the region containing the points $s\vec{v}, s \in (-1, t)$, and let B_t be the region containing the points $s\vec{v}, s \in (t, 1)$. Let $(M \cap A_t)'$ be the isometric reflection of $M \cap A_t$ across P_t .

Let t_0 be the largest value t_0 such that for all t less than t_0 , $\text{Int}((M \cap A_t)')$ and $\text{Int}(M \cap B_t)$ are disjoint. When t is close to -1 or 1, $P_t \cap M$ is empty, so it follows that such a t_0 exists and that $t_0 \in (-1, 1)$. It then follows (since M is properly embedded) that there exists a finite point of common tangency between $(M \cap A_{t_0})'$ and $M \cap B_{t_0}$, and that one surface lies above the other in a neighborhood of this point of common tangency. The maximum principle implies that $M \cap B_{t_0} = (M \cap A_{t_0})'$. (This is the Alexandrov reflection principle.) Since M has only two ends at the north and south poles, it must be that $t_0 = 0$. Since \vec{v} was an arbitrary horizontal vector, it follows that M is symmetric with respect to any geodesic plane through the north and south poles. Thus it is a surface of revolution.

If the surface M has no ends or only one point in its asymptotic boundary, one can similarly conclude that M is a surface of revolution (spheres and horospheres). \square

4 Immersed Counterexample

In sections 5 and 6, we give a rigorous proof of existence of the genus 1 catenoid cousin. However, since the proof itself does not enlighten the reader as to why it should exist, we give a motivation in this section for why we should expect this surface to exist.

As noted in section 2, it was shown in [RUY] that for any complete finite total curvature minimal surface in \mathbb{R}^3 which satisfies certain conditions, there exists a corresponding 1-parameter family of CMC 1 surfaces in \mathbb{H}^3 . So, in this sense, the set of CMC 1 surfaces in \mathbb{H}^3 is a larger set than the set of minimal surfaces in \mathbb{R}^3 . We now briefly sketch the ideas behind the result in [RUY]. We do not describe the method in detail, as the reader can refer to [RUY].

We start with a given minimal surface in \mathbb{R}^3 , and thus have a Riemann surface Σ and meromorphic functions f and g given to us by the Weierstrass representation for minimal surfaces in \mathbb{R}^3 (Lemma 2.1). We can use this same Σ and f and g in the hyperbolic Weierstrass representation (Lemma 2.2) to produce a CMC c surface in $\mathbb{H}^3(-c^2)$ for each real number c .

As $c \rightarrow 0$, the Poincare model for $\mathbb{H}^3(-c^2)$ (a ball in \mathbb{R}^3 with Euclidean radius $\frac{1}{|c|}$) converges to Euclidean space \mathbb{R}^3 , and these CMC c surfaces in $\mathbb{H}^3(-c^2)$ converge to the given minimal surface (in the sense of C^∞ uniform convergence on compact sets). Thus for c close to zero, we can think of compact regions of the CMC c surfaces in $\mathbb{H}^3(-c^2)$ as small deformations of compact regions of the given minimal surface in \mathbb{R}^3 .

If the given minimal surface in \mathbb{R}^3 is not simply-connected, then there is a question about whether the deformed CMC c surfaces in $\mathbb{H}^3(-c^2)$ are well-defined. This is the period problem. (The period problem being solvable essentially means that a certain set of equations $\text{Per}_j(\lambda_i) = 0$ can be solved with respect to certain parameters λ_i of the surface. This will be explained in detail in terms of an $SU(2)$ condition in the next section.) The minimal surface is assumed to have a "nondegeneracy" property, as defined in [RUY]. Since the period problem is nondegenerate and solvable on the minimal surface, and since the period problem changes continuously with respect to c , the period problem can still be solved when c is sufficiently close to 0. Thus, for c sufficiently close to 0, the CMC c surfaces in $\mathbb{H}^3(-c^2)$ are well-defined.

Dilating the Poincare model for $\mathbb{H}^3(-c^2)$ by a factor of $|c|$ (as described in section 2), we produce a one-parameter family of CMC 1 surfaces in \mathbb{H}^3 , with parameter c . This is the method used in [RUY] to create well-defined non-simply-connected CMC 1 surfaces in \mathbb{H}^3 from non-simply-connected minimal surfaces in \mathbb{R}^3 .

As an example of this, consider the minimal genus 1 trinoid in \mathbb{R}^3 . As discussed in [BR], there is a single real parameter λ in the Weierstrass data that can be adjusted to solve the period problem. The period problem is represented by a map $\lambda \in \mathbb{R} \rightarrow$

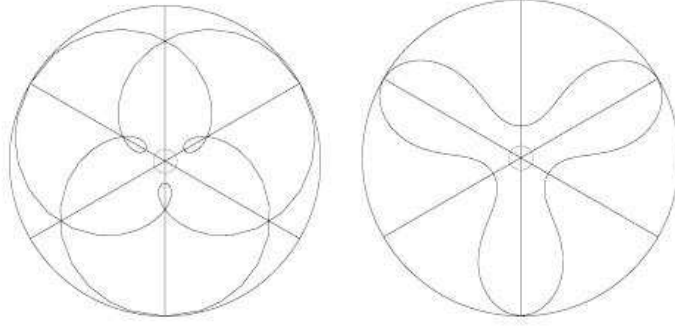


Figure 4: These are slices of genus 1 trinoid cousins along a plane of reflective symmetry. The lefthand picture is an embedded genus 1 trinoid cousin, produced by using a negative value for c . The righthand picture is an immersed genus 1 trinoid cousin, produced by using a positive value for c .

$\text{Per}(\lambda) \in \mathbb{R}$, and to solve the period problem we must show that there exists a value of λ so that $\text{Per}(\lambda) = 0$. We note that the function $\text{Per}(\lambda)$ changes continuously in c . Since the period problem for the minimal genus 1 trinoid in \mathbb{R}^3 (when c is 0) is solvable and nondegenerate, this implies that there exists an interval $(a, b) \in \mathbb{R}$ so that the image of this interval under the map Per contains an interval about 0. By continuity, if we perturb c slightly away from 0, it still holds that $0 \in \text{Per}((a, b))$. Thus, for c sufficiently close to zero, there exists a CMC c genus 1 trinoid cousin in $\mathbb{H}^3(-c^2)$. Then, by dilating the Poincare model, we produce a CMC 1 genus 1 trinoid cousin in $\mathbb{H}^3(-1)$ (see Figure 4).

Now let us consider Weierstrass data that would produce a minimal genus 1 catenoid in \mathbb{R}^3 . Again there is a single real parameter λ in the Weierstrass data that can be adjusted, and again the period problem is represented by a map $\lambda \in \mathbb{R} \rightarrow \text{Per}(\lambda) \in \mathbb{R}$, and to solve the period problem we must again show that there exists a value of λ so that $\text{Per}(\lambda) = 0$. The Weierstrass data is described in the next section. In this case the period problem cannot be solved, since the function Per is always positive, but the function Per can get arbitrarily close to 0. So we have that an interval $(0, \epsilon)$ is contained in the image of Per , for some $\epsilon > 0$. If we perturb c slightly, we expect that the image interval $(0, \epsilon)$ gets perturbed continuously. The authors have found by numerical experiment that when c becomes slightly negative, the image interval $(0, \epsilon)$ changes to an image interval of the form (ϵ_1, ϵ_2) , where $0 < \epsilon_1 < \epsilon_2$. Thus as c becomes negative, the lower endpoint of the image interval moves in a positive direction. If this behavior were nondegenerate at $c = 0$, then one would expect that as c is perturbed slightly in a positive direction, the image interval would become of the form (ϵ_1, ϵ_2) , where $\epsilon_1 < 0 < \epsilon_2$. We have found by numerical experiment that this is indeed the case. Thus for slightly positive values of c , we can adjust a real parameter in the Weierstrass data so that the period function Per becomes zero. Then, after dilating the Poincare model, we have existence of a CMC 1 genus 1 catenoid cousin in $\mathbb{H}^3(-1)$.

The behavior of the genus 1 catenoid as c is perturbed is similar to the behavior of the genus 1 trinoid as c is perturbed. As c becomes negative, the genus 1 trinoid cousin eventually becomes embedded. If the period problem could be solved for the genus 1 catenoid cousin when $c < 0$, the resulting surface would be embedded, but as we know by Theorem 1.1, such a surface cannot exist. But when solving the period problem for $c > 0$, the genus 1 catenoid cousin is not embedded, just in the same way that the genus 1 trinoid cousin is not embedded for $c > 0$. So this numerical experiment is consistent with Theorem 1.1, and furthermore shows that Theorem 1.1 holds only for embedded surfaces.

In the next sections, we will prove Theorem 1.2. First we describe the Weierstrass representation and the period problem. Then we give the proof. Initially the period problem is a three dimensional problem. We reduce the period problem by algebraic arguments to a one dimensional problem, then we show by a numerical calculation and the intermediate value theorem that this one dimensional period problem can be solved. The remainder of the proof is essentially a mathematically rigorous verification that the numerical experiment we conducted is correct. We must give mathematically rigorous bounds for both computer round-off error and for error introduced by discretizing the problem. We will show the errors are sufficiently small to ensure existence of a solution to the period problem.

5 Period Problem for the Genus 1 Catenoid Cousin

Consider the Riemann surface

$$\mathcal{M}_a^2 = \{(z, w) \in \mathbb{C} \times (\mathbb{C} \cup \{\infty\}) : (z-1)(z+a)w^2 = (z+1)(z-a)\}$$

for $a > 1$. Thus \mathcal{M}_a^2 is a twice punctured torus. Let $g = w$ and let $f = \frac{c}{w}$, for $c > 0$. (This c is the same as the c described in the previous section, and a is the same as λ in the previous section.) The Riemann surface \mathcal{M}_a^2 and meromorphic functions g and f are the Weierstrass data for a genus 1 catenoid. Let $F(z, w) \in SL(2, \mathbb{C})$ satisfy Bryant's equation

$$F^{-1}dF = \begin{pmatrix} g & -g^2 \\ 1 & -g \end{pmatrix} f dz$$

with initial condition $F(z=0, w=1) = \text{identity}$. Hence $\Phi = F^{-1}\overline{F^{-1}}^t$ is a CMC 1 surface in the Hermitean model for \mathbb{H}^3 , and this surface is defined on the universal cover of \mathcal{M}_a^2 . (Representing Φ in this way, we have already done the dilation of hyperbolic space which produces a CMC 1 surface in $\mathbb{H}^3(-1)$ from a CMC c surface in $\mathbb{H}^3(-c^2)$.)

However, we don't yet know that Φ is well-defined on \mathcal{M}_a^2 itself (which must be the case if Φ has finite total curvature $\int_{\mathcal{M}_a^2} -K dA < +\infty$). To have this, we need that F satisfies the $SU(2)$ condition, which we now describe. Suppose that γ is a loop in \mathcal{M}_a^2 with base point $p \in \mathcal{M}_a^2$. Suppose that the value of F at p is $F(p)$. Starting with the initial condition $F(p)$ and evaluating F along γ using Bryant's equation above,

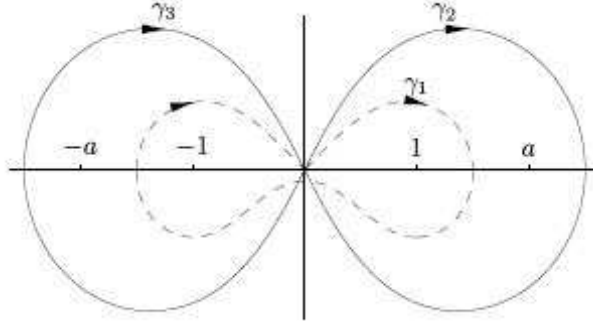


Figure 5: The curves γ_1 , γ_2 , and γ_3 generate the fundamental group of \mathcal{M}_a^2 .

we return to the base point p with a new value $\check{F}(p)$ for F at p . If the loop γ is nontrivial, we can expect that $\check{F}(p) \neq F(p)$. However, since both $\check{F}(p)$ and $F(p)$ are in $SL(2, \mathbb{C})$, there exists a matrix $P \in SL(2, \mathbb{C})$ such that $\check{F}(p) = P \cdot F(p)$. If $P \in SU(2)$, then it follows that $\check{F}^{-1} \check{F}^{-1^t} = F^{-1} \overline{F^{-1}}^t$. Thus if $P \in SU(2)$ for any loop γ , then Φ is well-defined on \mathcal{M}_a^2 itself. We say that the $SU(2)$ condition is satisfied on γ if $P \in SU(2)$.

It is enough to check the $SU(2)$ condition on the following three loops, as they generate the fundamental group of \mathcal{M}_a^2 (see Figure 5):

- Let $\gamma_1 \subset \mathcal{M}_a^2$ be a curve starting at $(0, 1) \in \mathcal{M}_a^2$ whose first portion has z coordinate in the first quadrant of the z plane and ends at a point (z, w) where $z \in \mathbb{R}$ and $1 < z < a$, and whose second portion starts at (z, w) and ends at $(0, -1)$ and has z coordinate in the second quadrant, and whose third portion starts at $(0, -1)$ and ends at $(-z, \frac{1}{w})$ and has z coordinate in the third quadrant, and whose fourth and last portion starts at $(-z, \frac{1}{w})$ and returns to the base point $(0, 1)$ and has z coordinate in the fourth quadrant.
- Let $\gamma_2 \subset \mathcal{M}_a^2$ be a curve starting at $(0, 1)$ whose first portion has z coordinate in the first quadrant and ends at a point (z, w) where $z \in \mathbb{R}$ and $z > a$, and whose second and last portion starts at (z, w) and returns to $(0, 1)$ and has z coordinate in the second quadrant.
- Let $\gamma_3 \subset \mathcal{M}_a^2$ be a curve starting at $(0, 1)$ whose first portion has z coordinate in the third quadrant and ends at a point (z, w) where $z \in \mathbb{R}$ and $z < -a$, and whose second and last portion starts at (z, w) and returns to $(0, 1)$ and has z coordinate in the fourth quadrant.

Consider the following symmetries from \mathcal{M}_a^2 to \mathcal{M}_a^2 : $\phi_1(z, w) = (\bar{z}, \bar{w})$, $\phi_2(z, w) = (-z, \frac{1}{w})$, $\phi_3(z, w) = (-\bar{z}, \frac{1}{\bar{w}})$. If $(z(t), w(t)), t \in [0, 1]$ is a curve in \mathcal{M}_a^2 that begins at $(0, 1)$ when $t = 0$ and ends at some point (z, w) when $t = 1$, then we can consider how F changes along $(z(t), w(t))$. At the beginning point of $(z(t), w(t))$ let $F(0, 1)$ be the identity, and denote the value of F at the ending point of $(z(t), w(t))$ by $F(z, w)$.

Then if we consider the curve $\phi_i(z(t), w(t))$, F is the identity at the beginning of this curve as well, and we denote the value of F at the end of this curve by $F(\phi_i(z, w))$. The following lemma gives the relationships between $F(z, w)$ and $F(\phi_i(z, w))$.

Lemma 5.1 *If $F(z, w) = \begin{pmatrix} A & B \\ C & D \end{pmatrix}$, then $F(\phi_1(z, w)) = \begin{pmatrix} \bar{A} & \bar{B} \\ \bar{C} & \bar{D} \end{pmatrix}$ and $F(\phi_2(z, w)) = \begin{pmatrix} D & C \\ B & A \end{pmatrix}$ and $F(\phi_3(z, w)) = \begin{pmatrix} \bar{D} & \bar{C} \\ \bar{B} & \bar{A} \end{pmatrix}$.*

Proof. Suppose $F(0, 1)$ is the identity and $F = \begin{pmatrix} A & B \\ C & D \end{pmatrix}$ is a solution to the equation

$$\begin{pmatrix} dA & dB \\ dC & dD \end{pmatrix} = \begin{pmatrix} A & B \\ C & D \end{pmatrix} \begin{pmatrix} 1 & -g \\ \frac{1}{g} & -1 \end{pmatrix} cdz$$

on $(z(t), w(t))$. Equivalently,

$$\begin{pmatrix} d\bar{A} & d\bar{B} \\ d\bar{C} & d\bar{D} \end{pmatrix} = \begin{pmatrix} \bar{A} & \bar{B} \\ \bar{C} & \bar{D} \end{pmatrix} \begin{pmatrix} 1 & -\bar{g} \\ \frac{1}{\bar{g}} & -1 \end{pmatrix} cd\bar{z}$$

on $(z(t), w(t))$. Since when $(z, w) \rightarrow \phi_1(z, w)$, we have that $z \rightarrow \bar{z}$ and $g \rightarrow \bar{g}$, we conclude that $\begin{pmatrix} \bar{A} & \bar{B} \\ \bar{C} & \bar{D} \end{pmatrix}$ is a solution on $\phi_1(z(t), w(t))$. Since the initial condition $F = \text{identity}$ is left unchanged by conjugation, we conclude the first part of the lemma. The above equation could also be equivalently written as

$$\begin{pmatrix} dD & dC \\ dB & dA \end{pmatrix} = \begin{pmatrix} D & C \\ B & A \end{pmatrix} \begin{pmatrix} 1 & -\frac{1}{g} \\ g & -1 \end{pmatrix} cd(-z).$$

Since when $(z, w) \rightarrow \phi_2(z, w)$, we have that $z \rightarrow -z$ and $g \rightarrow \frac{1}{g}$, we can conclude the second part of the lemma in the same way. Since $\phi_3 = \phi_2 \circ \phi_1$, the first two parts of the lemma imply the final part. \square

In the next lemma, we consider the map $\phi_4(z, w) = (\bar{z}, -\bar{w})$. This map is different from the other three maps $\phi_i(z, w)$, $i = 1, 2, 3$ in that $(0, 1)$ is not in the fixed point set of ϕ_4 . Thus when $(z(t), w(t))$ is a curve that begins at $(0, 1)$, $\phi_4(z(t), w(t))$ is a curve that begins at $(0, -1)$, not $(0, 1)$.

Lemma 5.2 *Suppose that $(z(t), w(t)) \subset \mathcal{M}_a^2$ is a curve that starts at $(0, 1)$ and ends at a point (z, w) such that $z \in \mathbb{R}$ and $1 < z < a$. Evaluating Bryant's equation along $(z(t), w(t))$ with initial condition $F(0, 1) = \text{identity}$, we denote the value of F at the endpoint (z, w) by $F(z, w) = \begin{pmatrix} A & B \\ C & D \end{pmatrix}$. Then $\phi_4(z(t), w(t))$ starts at $(0, -1)$ and ends at the same endpoint (z, w) . If we evaluate Bryant's equation along $\phi_4(z(t), w(t))$ with initial condition $F(0, -1) = \text{identity}$, then the value of F at the endpoint (z, w) of $\phi_4(z(t), w(t))$ is $F(\phi_4(z, w)) = \begin{pmatrix} \bar{A} & -\bar{B} \\ -\bar{C} & \bar{D} \end{pmatrix}$.*

Proof. Bryant's equation can be equivalently written as

$$\begin{pmatrix} d\bar{A} & -d\bar{B} \\ -d\bar{C} & d\bar{D} \end{pmatrix} = \begin{pmatrix} \bar{A} & -\bar{B} \\ -\bar{C} & \bar{D} \end{pmatrix} \begin{pmatrix} 1 & \bar{g} \\ -\frac{1}{\bar{g}} & -1 \end{pmatrix} cd\bar{z}.$$

The result follows just as in the previous proof. \square

Let $\alpha_1(t), t \in [0, 1]$ be a curve starting at $(z, w) = (0, 1)$ whose projection to the z -plane is an embedded curve in the first quadrant, and whose endpoint has a z coordinate that is real and larger than 1 and less than a . Let $\alpha_2(t), t \in [0, 1]$ be a curve starting at $(z, w) = (0, 1)$ whose projection to the z -plane is an embedded curve in the first quadrant, and whose endpoint has a z coordinate that is real and larger than a . With F =identity at $(z, w) = (0, 1)$, we solve Bryant's equation along these two paths to find that

$$F(\alpha_1(1)) = \begin{pmatrix} A_1 & B_1 \\ C_1 & D_1 \end{pmatrix}, \quad F(\alpha_2(1)) = \begin{pmatrix} A_2 & B_2 \\ C_2 & D_2 \end{pmatrix}.$$

Then traveling about the loop γ_1 , it follows from Lemmas 5.1 and 5.2 that F changes from the identity to the matrix

$$\phi := \begin{pmatrix} A_1 & B_1 \\ C_1 & D_1 \end{pmatrix} \begin{pmatrix} \bar{D}_1 & \bar{B}_1 \\ \bar{C}_1 & \bar{A}_1 \end{pmatrix} \begin{pmatrix} D_1 & -C_1 \\ -B_1 & A_1 \end{pmatrix} \begin{pmatrix} \bar{A}_1 & -\bar{C}_1 \\ -\bar{B}_1 & \bar{D}_1 \end{pmatrix}.$$

And traveling about the loop γ_2 , it follows from Lemma 5.1 that F changes from the identity to the matrix

$$\psi := \begin{pmatrix} A_2 & B_2 \\ C_2 & D_2 \end{pmatrix} \begin{pmatrix} \bar{D}_2 & -\bar{B}_2 \\ -\bar{C}_2 & \bar{A}_2 \end{pmatrix}.$$

And traveling about γ_3 , F changes from the identity to the matrix

$$\begin{pmatrix} D_2 & C_2 \\ B_2 & A_2 \end{pmatrix} \begin{pmatrix} \bar{A}_2 & -\bar{C}_2 \\ -\bar{B}_2 & \bar{D}_2 \end{pmatrix}.$$

Changing the initial condition from $F(0, 1) = \text{identity}$ to

$$F(0, 1) = \begin{pmatrix} \alpha & \beta \\ \beta & \alpha \end{pmatrix},$$

where $\alpha, \beta \in \mathbb{R}$, $\alpha^2 - \beta^2 = 1$, we see that solving the $SU(2)$ conditions on all three loops γ_1 , γ_2 , and γ_3 is equivalent to showing that

$$\begin{pmatrix} \alpha & \beta \\ \beta & \alpha \end{pmatrix} \phi \begin{pmatrix} \alpha & -\beta \\ -\beta & \alpha \end{pmatrix}, \quad \begin{pmatrix} \alpha & \beta \\ \beta & \alpha \end{pmatrix} \psi \begin{pmatrix} \alpha & -\beta \\ -\beta & \alpha \end{pmatrix}$$

are both in $SU(2)$. We can choose an α and β so that this holds precisely when

$$f_1 := \frac{-2(\bar{A}_1 D_1 + \bar{D}_1 A_1 + \bar{C}_1 B_1 + \bar{B}_1 C_1)}{\bar{D}_1 C_1 + \bar{C}_1 D_1 + \bar{B}_1 A_1 + \bar{A}_1 B_1} = \frac{2(\bar{A}_2 D_2 - \bar{D}_2 A_2 + \bar{C}_2 B_2 - \bar{B}_2 C_2)}{\bar{D}_2 C_2 - \bar{C}_2 D_2 + \bar{B}_2 A_2 - \bar{A}_2 B_2} =: f_2$$

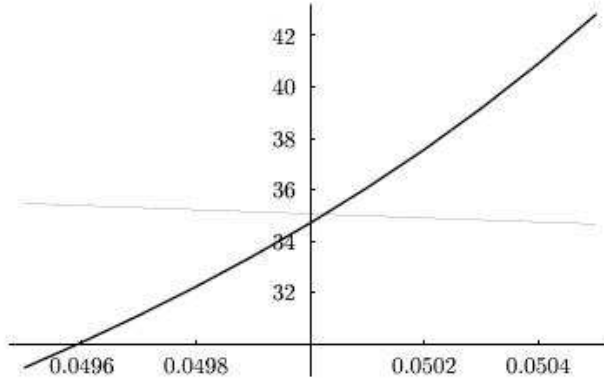


Figure 6: The functions f_1 (the gray curve) and f_2 (the black curve) when $a = 1.78$. The horizontal axis represents c , and the vertical axis represents f_1 and f_2 . We can see that $f_1, f_2 > 2$ on the interval $c \in (0.0495, 0.0505)$, and $f_1 = f_2$ at some value of c , and $a > 1$.

and the absolute value of this number is greater than 2. If this holds, we choose α and β so that

$$f_1 = \frac{1 + 2\beta^2}{\beta\sqrt{1 + \beta^2}} = f_2 \quad ,$$

and then the $SU(2)$ conditions are satisfied.

In order to prove Theorem 1.2, we need to show there exist values c and a so that $c > 0$, $a > 1$, $|f_1| = |f_2| > 2$, and $f_1 = f_2$. In this next section we check that such values for c and a exist, by doing a mathematically rigorous analysis of the error bounds for our numerical approximations. (See Figure 6.)

6 Error Estimates

Here we shall prove that for some given value of $a > 1$ there exists a positive value for c so that $f_1 = f_2 > 2$. We do this by showing that for one particular value for a , there exists a value of $c > 0$, call it c_1 , so that $f_1 > f_2$ at c_1 , and there exists another value of $c > c_1$, call it c_2 , so that $f_1 < f_2$ at c_2 . We also show that $+\infty > f_1, f_2 > 2$ for all values of $c \in (c_1, c_2)$. Then, by the continuity of f_i and the intermediate value theorem, we conclude that there exists a $c \in [c_1, c_2]$ such that $f_1 = f_2 > 2$.

Furthermore, by continuity, for any other value of a sufficiently close to our chosen value of a , there also exists a positive value for c so that $f_1 = f_2 > 2$, and hence the genus 1 catenoid exists for all a sufficiently close to our chosen value of a . Thus, with our method, showing existence for one value of a is sufficient to conclude the existence of a one-parameter family of genus 1 catenoid cousins. (However, we cannot draw any conclusions about the possible range of the parameter a for this one-parameter family.)

Thus, to prove Theorem 1.2, it is sufficient to do the following:

- We choose a suitable value for a and call it a_0 . Then we choose suitable values for $c_1 > 0$ and $c_2 > c_1$.
- Using the initial condition $F=\text{identity}$, and the value a_0 for a , and using the value c_i for c , we evaluate the Runge-Kutta algorithm approximation for the solution to Bryant's equation along the path $\alpha_j(t)$. With each evaluation of the Runge-Kutta algorithm, we make the evaluation by both rounding each mathematical operation upward and rounding each mathematical operation downward. Thus for each output of the algorithm, we can find a range in which the theoretical value of the output of the algorithm must lie.
- We then use Lemma 6.1, which gives an upper bound on the absolute value of the difference between the theoretical value of the output of the algorithm and the actual value of the solution of Bryant's equation. Using Lemma 6.1, we can find a single bound which is valid for $a = a_0$ and all $c \in [c_1, c_2]$.
- We then have enough information to determine that any possible approximation errors are small enough to ensure that at c_1 , $f_1 > f_2$ and that at c_2 , $f_1 < f_2$.
- Then, it only remains to show that f_1 and f_2 are both bounded and greater than 2 for all $c \in [c_1, c_2]$. We do this by showing that the derivative with respect to c of the theoretical value of the output of the algorithm is bounded by a certain constant, for all $c \in [c_1, c_2]$. This is the purpose of Lemma 6.2 – it allows us to place limits on the rate at which the output of the algorithm can change with respect to c . This enables us to conclude that $2 < f_i < \infty$ for all $c \in [c_1, c_2]$ simply by checking that this is so at a finite number of values of c in $[c_1, c_2]$.

Lemma 6.1 *Let $\alpha(t), t \in [0, 1]$ be a path in the complex plane. Let*

$$F(\alpha(t)) = \begin{pmatrix} A(t) & B(t) \\ C(t) & D(t) \end{pmatrix}$$

be an $SL(2, \mathbb{C})$ -valued function on $\alpha(t)$ such that $F(\alpha(0))=\text{identity}$ and $F(\alpha(t))$ satisfies the equation

$$\begin{pmatrix} \frac{dA}{dt} & \frac{dB}{dt} \\ \frac{dC}{dt} & \frac{dD}{dt} \end{pmatrix} = \begin{pmatrix} A & B \\ C & D \end{pmatrix} \begin{pmatrix} ch_1 & ch_3 \\ ch_2 & ch_4 \end{pmatrix},$$

where c is a real positive constant and h_i are functions on the complex plane satisfying the bounds $|h_i| < M$, $|h'_i| < M_1$, $|h''_i| < M_2$, $|h'''_i| < M_3$ on $\alpha(t)$ for $i = 1, 2, 3, 4$. Assume also that h_1 and h_4 are constant functions, and choose $n \in \mathbb{Z}^+$ so that $\frac{Mc}{n} < \frac{1}{100}$. Applying the standard Runge-Kutta algorithm on the interval $t \in [0, 1]$,

using n equally lengthed intervals, let the resulting approximate value for $F(\alpha(1))$ produced by the Runge-Kutta algorithm be denoted by the matrix

$$\begin{pmatrix} \tilde{A} & \tilde{B} \\ \tilde{C} & \tilde{D} \end{pmatrix}.$$

Then $|A(1)-\tilde{A}|$, $|B(1)-\tilde{B}|$, $|C(1)-\tilde{C}|$, and $|D(1)-\tilde{D}|$ are all bounded by $\frac{e^{2.1cM}+e^{4.1cM}}{4.2cMn^{12}}\zeta$, where ζ is the following polynomial:

$$\begin{aligned} \zeta(c, n, M, M_1, M_2, M_3) = & \frac{n^9 c}{72}(96c^3 M^4 + 144c^2 M^2 M_1 + 18cM_1^2 + 48cMM_2 + 13M_3) + \\ & \frac{n^8 c^2}{48}(32c^2 M^3 M_1 + 12cMM_1^2 + 16cM^2 M_2 + 4M_1 M_2 + 11MM_3) + \\ & \frac{n^7 c^2}{384}(80c^2 M^2 M_1^2 + 8cM_1^3 + 96c^2 M^3 M_2 + 64cMM_1 M_2 + 5M_2^2 + 79cM^2 M_3 + 22M_1 M_3) + \\ & \frac{n^6 c^2}{2304}(48c^2 MM_1^3 + 336c^2 M^2 M_1 M_2 + 48cM_1^2 M_2 + 60cMM_2^2 + 272c^2 M^3 M_3 + 236cMM_1 M_3 + \\ & 49M_2 M_3) + \frac{n^5 c^2}{2304}(48c^2 MM_1^2 M_2 + \\ & 54c^2 M^2 M_2^2 + 15cM_1 M_2^2 + 200c^2 M^2 M_1 M_3 + 26cM_1^2 M_3 + 84cMM_2 M_3 + 12M_3^2) + \\ & \frac{n^4 c^3}{13824}(90cMM_1 M_2^2 + 9M_2^3 + 156cMM_1^2 M_3 + 450cM^2 M_2 M_3 + 105M_1 M_2 M_3 + 116MM_3^2) + \\ & \frac{n^3 c^3}{27648}(18cMM_2^3 + 210cMM_1 M_2 M_3 + 33M_2^2 M_3 + 216cM^2 M_3^2 + 44M_1 M_3^2) + \\ & \frac{n^2 c^3}{27648}(33cMM_2^2 M_3 + 44cMM_1 M_3^2 + 13M_2 M_3^2) + \frac{nc^3}{82944}(39cMM_2 M_3^2 + 4M_3^3) + \frac{c^4}{20736}MM_3^3. \end{aligned}$$

We include the condition that h_1 and h_4 are constant in Lemma 6.1, because this is sufficient for our application, and this will later allow us to assume a smaller lower bound for n . It also simplifies the proof somewhat. However, it is not necessary to assume h_1 and h_4 are constant in order to produce a lemma of this type.

Proof. The system of equations in the lemma can be separated into two systems of two equations each – one the systems with variables A and B , and the other with C and D . We consider now the system involving A and B :

$$\frac{dA}{dt} = ch_1 A + ch_2 B, \quad \frac{dB}{dt} = ch_3 A + ch_4 B.$$

Since $|h_i| < M$ for all $t \in [0, 1]$ and all $i = 1, 2, 3, 4$, we conclude that

$$\left| \frac{dA}{dt} \right| \leq cM|A| + cM|B|, \quad \left| \frac{dB}{dt} \right| \leq cM|A| + cM|B|.$$

If we replace the inequalities in these equations by equalities, we would be able to evaluate the system explicitly with $A(0) = 1$ and $B(0) = 0$. It follows that

$$|A(t)| \leq 1 + \frac{1}{2} \sum_{j=1}^{\infty} \frac{(2tcM)^j}{j!} = \frac{1}{2} + \frac{1}{2} e^{2tcM} \quad , \quad |B(t)| \leq \frac{1}{2} \sum_{j=1}^{\infty} \frac{(2tcM)^j}{j!} = -\frac{1}{2} + \frac{1}{2} e^{2tcM} \quad .$$

Now we run the standard Runge-Kutta algorithm on $t \in [0, 1]$ for a system of two equations with n steps of equal size $\frac{1}{n}$. The initial conditions are $A_0 = 1$ and $B_0 = 0$. The algorithm at step k is this:

$$\begin{aligned} k_0 &= \frac{c}{n} (h_1(\frac{k}{n})A_k + h_2(\frac{k}{n})B_k) \quad , \quad m_0 = \frac{c}{n} (h_3(\frac{k}{n})A_k + h_4(\frac{k}{n})B_k) \quad , \\ k_1 &= \frac{c}{n} (h_1(\frac{k}{n} + \frac{1}{2n})(A_k + \frac{1}{2}k_0) + h_2(\frac{k}{n} + \frac{1}{2n})(B_k + \frac{1}{2}m_0)) \quad , \\ m_1 &= \frac{c}{n} (h_3(\frac{k}{n} + \frac{1}{2n})(A_k + \frac{1}{2}k_0) + h_4(\frac{k}{n} + \frac{1}{2n})(B_k + \frac{1}{2}m_0)) \quad , \\ k_2 &= \frac{c}{n} (h_1(\frac{k}{n} + \frac{1}{2n})(A_k + \frac{1}{2}k_1) + h_2(\frac{k}{n} + \frac{1}{2n})(B_k + \frac{1}{2}m_1)) \quad , \\ m_2 &= \frac{c}{n} (h_3(\frac{k}{n} + \frac{1}{2n})(A_k + \frac{1}{2}k_1) + h_4(\frac{k}{n} + \frac{1}{2n})(B_k + \frac{1}{2}m_1)) \quad , \\ k_3 &= \frac{c}{n} (h_1(\frac{k}{n} + \frac{1}{n})(A_k + k_2) + h_2(\frac{k}{n} + \frac{1}{n})(B_k + m_2)) \quad , \\ m_3 &= \frac{c}{n} (h_3(\frac{k}{n} + \frac{1}{n})(A_k + k_2) + h_4(\frac{k}{n} + \frac{1}{n})(B_k + m_2)) \quad , \\ A_{k+1} &= A_k + \frac{1}{6}(k_0 + 2k_1 + 2k_2 + k_3) \quad , \quad B_{k+1} = B_k + \frac{1}{6}(m_0 + 2m_1 + 2m_2 + m_3) \quad . \end{aligned}$$

We define the local discretization errors for A and B to be

$$\begin{aligned} d_{k+1}^A &:= A(\frac{k+1}{n}) - A(\frac{k}{n}) - \frac{1}{6}(\hat{k}_0 + 2\hat{k}_1 + 2\hat{k}_2 + \hat{k}_3) \quad , \\ d_{k+1}^B &:= B(\frac{k+1}{n}) - B(\frac{k}{n}) - \frac{1}{6}(\hat{m}_0 + 2\hat{m}_1 + 2\hat{m}_2 + \hat{m}_3) \quad , \end{aligned}$$

where

$$\begin{aligned} \hat{k}_0 &= \frac{c}{n} (h_1(\frac{k}{n})A(\frac{k}{n}) + h_2(\frac{k}{n})B(\frac{k}{n})) \quad , \quad \hat{m}_0 = \frac{c}{n} (h_3(\frac{k}{n})A(\frac{k}{n}) + h_4(\frac{k}{n})B(\frac{k}{n})) \quad , \\ \hat{k}_1 &= \frac{c}{n} (h_1(\frac{k}{n} + \frac{1}{2n})(A(\frac{k}{n}) + \frac{1}{2}\hat{k}_0) + h_2(\frac{k}{n} + \frac{1}{2n})(B(\frac{k}{n}) + \frac{1}{2}\hat{m}_0)) \quad , \end{aligned}$$

and $\hat{m}_1, \hat{k}_2, \hat{m}_2, \hat{k}_3, \hat{m}_3$ are defined similarly, analogous to the way m_1, k_2, m_2, k_3, m_3 were defined. We define the maximums of the local discretization errors by

$$D^A := \max_k |d_k^A| \quad , \quad D^B := \max_k |d_k^B| \quad , \quad D := \max(D^A, D^B) \quad .$$

We define the global discretization errors by

$$g_k^A := A\left(\frac{k}{n}\right) - A_k \quad , \quad g_k^B := B\left(\frac{k}{n}\right) - B_k \quad , \quad g_k := \max(|g_k^A|, |g_k^B|) \quad .$$

Since $A(\frac{k+1}{n}) = A(\frac{k}{n}) + \frac{1}{6}(\hat{k}_0 + 2\hat{k}_1 + 2\hat{k}_2 + \hat{k}_3) + d_{k+1}^A$, we have that

$$g_{k+1}^A = g_k^A + \frac{1}{6}(\hat{k}_0 + 2\hat{k}_1 + 2\hat{k}_2 + \hat{k}_3) - \frac{1}{6}(k_0 + 2k_1 + 2k_2 + k_3) + d_{k+1}^A \quad ,$$

and therefore we can compute that

$$\begin{aligned} |g_{k+1}^A| &\leq |g_k^A| + \left(\frac{cM}{n} + \frac{c^2M^2}{n^2} + \frac{2c^3M^3}{3n^3} + \frac{c^4M^4}{3n^4}\right) |A\left(\frac{k}{n}\right) - A_k| + \\ &\quad \left(\frac{cM}{n} + \frac{c^2M^2}{n^2} + \frac{2c^3M^3}{3n^3} + \frac{c^4M^4}{3n^4}\right) |B\left(\frac{k}{n}\right) - B_k| + |d_{k+1}^A| \quad . \end{aligned}$$

We assumed that $n > 100cM$, so we have

$$|g_{k+1}^A| \leq \left(1 + \frac{1.05cM}{n}\right) |g_k^A| + \frac{1.05cM}{n} |g_k^B| + D^A \quad .$$

Similarly,

$$|g_{k+1}^B| \leq \frac{1.05cM}{n} |g_k^A| + \left(1 + \frac{1.05cM}{n}\right) |g_k^B| + D^B \quad .$$

Thus,

$$g_{k+1} \leq \left(1 + \frac{2.1cM}{n}\right) g_k + D \quad .$$

By repeated application of this inequality we have

$$g_n \leq \left(1 + \frac{2.1cM}{n}\right)^n g_0 + \frac{(1 + \frac{2.1cM}{n})^n - 1}{\frac{2.1cM}{n}} D \quad .$$

And since $g_0 = 0$, we have

$$g_n \leq \frac{e^{\frac{2.1cMn}{n}} - 1}{\frac{2.1cM}{n}} D < \frac{ne^{2.1cM}}{2.1cM} D \quad .$$

Here we have used the fact that e^x is convex on \mathbb{R} and therefore $1 + x \leq e^x$ and therefore also $(1 + x)^n \leq (e^x)^n = e^{xn}$ for any positive x .

Note that $h_i(\frac{k}{n} + \frac{1}{2n})$ and $h_i(\frac{k}{n} + \frac{1}{n})$ and $A(\frac{k}{n} + \frac{1}{n})$ have the following Taylor expansions:

$$h_i\left(\frac{k}{n} + \frac{1}{2n}\right) = h_i\left(\frac{k}{n}\right) + \frac{1}{2n}h_i'\left(\frac{k}{n}\right) + \frac{1}{8n^2}h_i''\left(\frac{k}{n}\right) + \frac{1}{48n^3}h_i'''\left(\frac{k}{n} + \theta\frac{1}{2n}\right) \quad ,$$

$$h_i\left(\frac{k}{n} + \frac{1}{n}\right) = h_i\left(\frac{k}{n}\right) + \frac{1}{n}h_i'\left(\frac{k}{n}\right) + \frac{1}{2n^2}h_i''\left(\frac{k}{n}\right) + \frac{1}{6n^3}h_i'''\left(\frac{k}{n} + \theta\frac{1}{n}\right) \quad ,$$

$$A\left(\frac{k}{n} + \frac{1}{n}\right) = A\left(\frac{k}{n}\right) + \frac{1}{n}A'\left(\frac{k}{n}\right) + \frac{1}{2n^2}A''\left(\frac{k}{n}\right) + \frac{1}{6n^3}A'''\left(\frac{k}{n}\right) + \frac{1}{24n^4}A''''\left(\frac{k}{n} + \theta\frac{1}{n}\right),$$

for some values of $\theta \in [0, 1]$. Here the symbol $'$ denotes derivative with respect to t .

Repeatedly using that $A' = ch_1A + ch_2B$ and $B' = ch_3A + ch_4B$, the above Taylor expansion for $A(\frac{k}{n} + \frac{1}{n})$ can be rewritten in a longer form so that it does not contain any terms of the form $A', B', A'', B'', A''', B''', A''''$, or B'''' . Using this longer form for $A(\frac{k}{n} + \frac{1}{n})$, and using the above Taylor expansions for $h_i(\frac{k}{n} + \frac{1}{2n})$ and $h_i(\frac{k}{n} + \frac{1}{n})$, we can make a direct (but long) calculation to determine d_{k+1}^A and d_{k+1}^B in terms of A, B, n, c, h_i , and the derivatives (up to third order) of h_i . These formulas are extremely long, so we do not include them here. However, for each of these formulas we can take the sum of the absolute values of all of the terms, and make the following replacements: $|h_i|$ by its upper bound M , $|h'_i|$ by its upper bound M_1 , $|h''_i|$ by its upper bound M_2 , $|h'''_i|$ by its upper bound M_3 , and $|A|$ and $|B|$ by their upper bound $\frac{1+e^{2cM}}{2}$. We then get upper bounds for $|d_{k+1}^A|$ and $|d_{k+1}^B|$. We can then find that a sufficient upper bound for both $|d_{k+1}^A|$ and $|d_{k+1}^B|$ is $D \leq \frac{1+e^{2cM}}{2n^{13}}\zeta$. So we have that

$$g_n < \frac{ne^{2.1cM}}{2.1cM}D \leq \frac{ne^{2.1cM}}{2.1cM} \frac{1+e^{2cM}}{2n^{13}}\zeta.$$

An identical argument gives the same conclusion for C and D . \square

Lemma 6.2 *Suppose that the conditions of Lemma 6.1 hold for all c contained in some interval $[c_1, c_2]$. Then $|\frac{\partial \hat{A}}{\partial c}|$, $|\frac{\partial \hat{B}}{\partial c}|$, $|\frac{\partial \hat{C}}{\partial c}|$, and $|\frac{\partial \hat{D}}{\partial c}|$ are all bounded by $2.48Me^{2.4Mc}$ for all $c \in [c_1, c_2]$.*

Proof. We consider the system of two equations for A and B here. The case for C and D is identical.

Recall that the Runge-Kutta algorithm is

$$A_{j+1} = A_j + \frac{1}{6}(k_0 + 2k_1 + 2k_2 + k_3), \quad B_{j+1} = B_j + \frac{1}{6}(m_0 + 2m_1 + 2m_2 + m_3).$$

We can expand out the terms of these two equations so that everything is written in terms of only $A_j, B_j, A_{j+1}, B_{j+1}$ and h_i, c, n . We then have

$$A_{j+1} = A_j + \mathcal{Q}A_j + \mathcal{Q}B_j, \quad B_{j+1} = B_j + \mathcal{Q}A_j + \mathcal{Q}B_j,$$

where \mathcal{Q} is a polynomial that consists of the sum of two terms of the form $\frac{ch_*(*)}{6n}$, two terms of the form $\frac{ch_*(*)}{3n}$, six terms of the form $\frac{c^2h_*(*)h_*(*)}{6n^2}$, eight terms of the form $\frac{c^3h_*(*)h_*(*)h_*(*)}{12n^3}$, and eight terms of the form $\frac{c^4h_*(*)h_*(*)h_*(*)h_*(*)}{24n^4}$. We will use the symbol \mathcal{Q} to notate any polynomial of this form, regardless of what the subindices are for the functions $h_i(z)$ and regardless of at which value of $z(t)$ we are evaluating the functions $h_i(z)$. (It is for this reason that we are notating the functions $h_i(z)$ merely as $h_*(*)$.) Although \mathcal{Q} is not a well-defined notation, for our purposes this level of notation will be sufficient. It follows from the assumptions $|h_i| < M$ and $c > 0$ and

$\frac{Mc}{n} < \frac{1}{100}$ that $|\mathcal{Q}| < 1.2\frac{Mc}{n}$ and $|\frac{\partial \mathcal{Q}}{\partial c}| < \frac{M}{n}(1 + 2.4\frac{Mc}{n})$, regardless of what the indices of h_i are and regardless of at which values of $z(t)$ we evaluate the functions h_i .

Applying the Runge-Kutta algorithm on n equally lengthed steps, we find that the resulting estimates for A and B at $\alpha(1)$ are of the form

$$A_n = A_0 + p(\mathcal{Q})A_0 + p(\mathcal{Q})B_0, \quad B_n = B_0 + p(\mathcal{Q})A_0 + p(\mathcal{Q})B_0,$$

where $p(\mathcal{Q})$ is a polynomial in \mathcal{Q} with $\frac{2^{j-1}n(n-1)(n-2)\cdots(n-j+1)}{j!}$ terms of the form \mathcal{Q}^j for each $j = 1, \dots, n$. Thus it follows that

$$\begin{aligned} \left| \frac{\partial A_n}{\partial c} \right|, \left| \frac{\partial B_n}{\partial c} \right| &\leq 2 \sum_{j=1}^n \frac{2^{j-1}n(n-1)(n-2)\cdots(n-j+1)}{j!} \left| \frac{\partial}{\partial c}(\mathcal{Q}^j) \right| \leq \\ &\sum_{j=1}^n \frac{2^j n(n-1)(n-2)\cdots(n-j+1)}{j!} j |\mathcal{Q}|^{j-1} \left| \frac{\partial \mathcal{Q}}{\partial c} \right| \leq \\ &\sum_{j=1}^n \frac{2^j n(n-1)(n-2)\cdots(n-j+1)}{j!} j \left(1.2\frac{Mc}{n}\right)^{j-1} \left(\frac{M}{n}(1 + 2.4\frac{Mc}{n})\right) \leq \\ &\sum_{j=1}^n \frac{2^j}{(j-1)!} (1.2Mc)^{j-1} (M(1 + 2.4\frac{Mc}{n})) \leq 2M(1 + 2.4\frac{Mc}{n}) \sum_{j=1}^n \frac{1}{(j-1)!} (2.4Mc)^{j-1} < \\ &2.48M \sum_{j=0}^{n-1} \frac{1}{j!} (2.4Mc)^j < 2.48M \sum_{j=0}^{\infty} \frac{1}{j!} (2.4Mc)^j = 2.48Me^{2.4Mc}. \end{aligned}$$

□

We are now in a position to prove Theorem 1.2:

Proof. Recall that our surface is described by the equation

$$\begin{pmatrix} \frac{dA}{dz} & \frac{dB}{dz} \end{pmatrix} = \begin{pmatrix} A & B \\ C & D \end{pmatrix} \begin{pmatrix} g & -g^2 \\ 1 & -g \end{pmatrix} \frac{c}{g},$$

where $g = \sqrt{\frac{(z+1)(z-a)}{(z-1)(z+a)}}$. This system separates into two systems – one involving A and B , and the other involving C and D . We consider now the system involving A and B :

$$\frac{dA}{dz} = cA + \frac{c}{g}B, \quad \frac{dB}{dz} = -cgA - cB.$$

Note that if we wish to evaluate this system along a curve from z_0 to z_1 , linearly defined as $\frac{b-t}{b-a}z_0 + \frac{t-a}{b-a}z_1$, $t \in [a, b]$, then $\frac{dz}{dt} = \frac{z_1-z_0}{b-a}$ for all $t \in [a, b]$. So our system can then be written as

$$\frac{dA}{dt} = c \frac{z_1-z_0}{b-a} A + c \frac{z_1-z_0}{b-a} \frac{1}{g} B, \quad \frac{dB}{dt} = -c \frac{z_1-z_0}{b-a} g A - c \frac{z_1-z_0}{b-a} B.$$

Let $h_1 = \frac{z_1-z_0}{b-a}$, $h_2 = \frac{z_1-z_0}{b-a} \frac{1}{g}$, $h_3 = -\frac{z_1-z_0}{b-a} g$, and $h_4 = -\frac{z_1-z_0}{b-a}$.

Now we choose the paths $\alpha_1(t)$ and $\alpha_2(t)$ for $t \in [0, 1]$. The paths will start at the point $\alpha_1(0) = \alpha_2(0) = (0, 1)$ in the base Riemann surface \mathcal{M}_a^2 and will be defined by their z coordinates. The z coordinates of the paths will be polygonal and t will be defined linearly with respect to z -length on each line segment. The path $\alpha_1(t)$ will project to a line segment from $z = 0$ ($t = 0$) to $z = 1 + 0.4i$ ($t = 0.67$), then a line segment from $z = 1 + 0.4i$ ($t = 0.67$) to $z = \frac{1}{2}(1 + a)$ ($t = 1$). The path $\alpha_2(t)$ will project to a line segment from $z = 0$ ($t = 0$) to $z = (a + 0.2) + 0.7i$ ($t = 0.686$), then a line segment from $z = (a + 0.2) + 0.7i$ ($t = 0.686$) to $z = a + \frac{1}{2}$ ($t = 1$).

We now solve Bryants differential equation along $\alpha_j(t)$. At the beginning point $(z, w) = (0, 1)$, that is, at $t = 0$, the initial condition will be $F = \text{identity}$. Suppose that the true value of F at the endpoints is

$$F(\alpha_j(1)) = \begin{pmatrix} A_j & B_j \\ C_j & D_j \end{pmatrix}, \quad j = 1, 2,$$

and suppose that the approximate value of F at the endpoints produced by the Runge-Kutta algorithm using n steps of equal length is

$$\begin{pmatrix} \tilde{A}_j & \tilde{B}_j \\ \tilde{C}_j & \tilde{D}_j \end{pmatrix}, \quad j = 1, 2.$$

Of course, the exact values of $\tilde{A}_j, \tilde{B}_j, \tilde{C}_j, \tilde{D}_j$ cannot be computed on a computer, but by considering the possible round-off error for each mathematical operation in the algorithm, and keeping track of the possible cumulative round-off error, we can find intervals in which the values $\tilde{A}_j, \tilde{B}_j, \tilde{C}_j, \tilde{D}_j$ must lie. That is, we can find real values $\tilde{A}_j^{ur}, \tilde{A}_j^{ui}, \tilde{A}_j^{lr}, \tilde{A}_j^{li}, \tilde{B}_j^{ur}, \tilde{B}_j^{ui}, \tilde{B}_j^{lr}, \tilde{B}_j^{li}, \tilde{C}_j^{ur}, \tilde{C}_j^{ui}, \tilde{C}_j^{lr}, \tilde{C}_j^{li}, \tilde{D}_j^{ur}, \tilde{D}_j^{ui}, \tilde{D}_j^{lr}, \tilde{D}_j^{li}$ such that

$$\tilde{\mathcal{I}}_j^{lr} \leq \text{Re}(\tilde{\mathcal{I}}_j) \leq \tilde{\mathcal{I}}_j^{ur}, \quad \tilde{\mathcal{I}}_j^{li} \leq \text{Im}(\tilde{\mathcal{I}}_j) \leq \tilde{\mathcal{I}}_j^{ui},$$

for $\mathcal{I} = A, B, C, D$ and $j = 1, 2$, thus giving us a total of 16 equations. (These bounds can be computed using code written in a programming language such as C++ or Fortran. They also could be computed using a shorter code written in a scientific programming language such as CXSC or PROFIL.) To explain why we write the superscripts in this way, the first letter is either u or l to denote either upper bound or lower bound, and the second letter is either r or i to denote either real part or imaginary part.

Choosing a to be 1.78, we find that we have the following bounds for both paths: $M = 4.6$, $M_1 = 48$, $M_2 = 850$, $M_3 = 25000$. (These bounds are defined in Lemma 6.1.) Then, if we choose any $c \in [0.0495, 0.0505]$, from Lemma 6.1 we see that if $n > 500$, the errors incurred by the Runge-Kutta algorithm on A_j, B_j, C_j , and D_j are less than $\epsilon = 0.00001$. That is, $|\tilde{A}_j - A_j| < \epsilon$, $|\tilde{B}_j - B_j| < \epsilon$, $|\tilde{C}_j - C_j| < \epsilon$, and $|\tilde{D}_j - D_j| < \epsilon$, for all $c \in [0.0495, 0.0505]$. It follows that

$$\tilde{\mathcal{I}}_j^{lr} - \epsilon \leq \text{Re}(\mathcal{I}_j) \leq \tilde{\mathcal{I}}_j^{ur} + \epsilon, \quad \tilde{\mathcal{I}}_j^{li} - \epsilon \leq \text{Im}(\mathcal{I}_j) \leq \tilde{\mathcal{I}}_j^{ui} + \epsilon,$$

for $\mathcal{I} = A, B, C, D$ and $j = 1, 2$.

The value of a is fixed, but c can be any value in the range $[0.0495, 0.0505]$, so the numbers $A_j, \dots, D_j, \tilde{A}_j, \dots, \tilde{D}_j, \tilde{A}_j^{ur}, \dots, \tilde{D}_j^{li}$ are all functions of c . To clearly show this dependence, we shall denote these numbers by $A_j(c), \dots, D_j(c), \tilde{A}_j(c), \dots, \tilde{D}_j(c), \tilde{A}_j^{ur}(c), \dots, \tilde{D}_j^{li}(c)$ for the rest of this proof.

By Lemma 6.2, $|\frac{\partial \tilde{A}_j(c)}{\partial c}|, |\frac{\partial \tilde{B}_j(c)}{\partial c}|, |\frac{\partial \tilde{C}_j(c)}{\partial c}|$, and $|\frac{\partial \tilde{D}_j(c)}{\partial c}|$ are all bounded by $2.48Me^{2.4Mc} < 20$ for all $c \in [0.0495, 0.0505]$. So, it follows that if we choose any $c \in [0.04999, 0.05001]$, we have that $\tilde{A}_j(c), \tilde{B}_j(c), \tilde{C}_j(c)$, and $\tilde{D}_j(c)$ can vary from their values at $c = 0.05$ by at most $\hat{\epsilon} = 0.0002$. That is, $|\tilde{A}_j(c) - \tilde{A}_j(0.05)| < \hat{\epsilon}$, $|\tilde{B}_j(c) - \tilde{B}_j(0.05)| < \hat{\epsilon}$, $|\tilde{C}_j(c) - \tilde{C}_j(0.05)| < \hat{\epsilon}$, and $|\tilde{D}_j(c) - \tilde{D}_j(0.05)| < \hat{\epsilon}$, for all $c \in [0.04999, 0.05001]$. We conclude that

$$\tilde{\mathcal{I}}_j^{lr}(0.05) - \epsilon - \hat{\epsilon} \leq \operatorname{Re}(\mathcal{I}_j(c)) \leq \tilde{\mathcal{I}}_j^{ur}(0.05) + \epsilon + \hat{\epsilon} ,$$

$$\tilde{\mathcal{I}}_j^{li}(0.05) - \epsilon - \hat{\epsilon} \leq \operatorname{Im}(\mathcal{I}_j(c)) \leq \tilde{\mathcal{I}}_j^{ui}(0.05) + \epsilon + \hat{\epsilon} ,$$

for $\mathcal{I} = A, B, C, D$ and $j = 1, 2$ and all $c \in [0.04999, 0.05001]$. This is sufficient to conclude that both $f_1, f_2 \in (2, +\infty)$ for all $c \in [0.04999, 0.05001]$. Checking in this way on many small intervals (a finite number of intervals), we can conclude that $2 < f_1, f_2 < \infty$ for all $c \in [0.0495, 0.0505]$.

Then, as we saw before, solving the period problem means solving $f_1 = f_2 > 2$. Running the Runge-Kutta algorithm with $c = 0.0495$, we conclude that

$$\tilde{\mathcal{I}}_j^{lr}(0.0495) - \epsilon \leq \operatorname{Re}(\mathcal{I}_j(0.0495)) \leq \tilde{\mathcal{I}}_j^{ur}(0.0495) + \epsilon ,$$

$$\tilde{\mathcal{I}}_j^{li}(0.0495) - \epsilon \leq \operatorname{Im}(\mathcal{I}_j(0.0495)) \leq \tilde{\mathcal{I}}_j^{ui}(0.0495) + \epsilon ,$$

for $\mathcal{I} = A, B, C, D$ and $j = 1, 2$. These estimates are sufficient to show that $f_1 > f_2$ at $c = 0.0495$. Similarly we can show that $f_1 < f_2$ at $c = 0.0505$. We conclude that there exists a value of $c \in [0.0495, 0.0505]$ so that $f_1 = f_2 > 2$. We have thus shown of existence of at least one genus 1 catenoid cousin. Then, since the problem is continuous in a , we know that for all a sufficiently close to 1.78 there exists a positive value for c so that $f_1 = f_2 > 2$. This proves existence of a one-parameter family of genus 1 catenoid cousins. \square

References

- [B] R. Bryant. Surfaces of Mean Curvature One in Hyperbolic Space. *Astérisque*, 154-155 (1987), 321-347.
- [BR] J. Berglund, and W. Rossmann. Minimal Surfaces with Catenoid Ends. *Pacific J. Math.*, 171 (1995), 353-371.
- [CL] M. P. do Carmo, and H. B. Lawson, Jr. On Alexandrov-Bernstein Theorems in Hyperbolic Space. *Duke Math. Journal*, 50 (1983), 995-1003.

- [CGT] M. P. do Carmo, J. M. Gomes, and G. Thorbergsson. The influence of the boundary behavior on hypersurfaces with constant mean curvature in \mathbb{H}^{n+1} . *Comm. Math. Helvetici*, 61 (1986), 429-441.
- [ER] R. Sa Earp, and H. Rosenberg. Some Remarks on Surfaces of Prescribed Mean Curvature. *Differential Geometry*, Pitman Monographs and Surveys in Pure and Applied Mathematics, vol. 52 (1991).
- [HHS] J. Hass, M. Hutchings, and R. Schlafly. The double bubble conjecture. *Electron. Res. Announc. Amer. Math. Soc.*, vol 1, no 3, (1995), p98-102.
- [K] N. Kapouleas, Complete Constant Mean Curvature Surfaces in Euclidean Three Space, *Ann. of Math.* 131 (1990), 239-330.
- [Kar] H. Karcher. The triply periodic minimal surfaces of A. Schoen and their constant mean curvature companions. *Man. Math.*, vol. 64, p291-357 (1989).
- [KPS] H. Karcher, U. Pinkall, and I. Sterling. New minimal surfaces in S^3 . *J. Diff. Geom.*, vol. 28, p169-185 (1988).
- [KKMS] N. Korevaar, R. Kusner, W. Meeks, and B. Solomon. Constant Mean Curvature Surfaces in Hyperbolic Space. *American J. Math.*, 114 (1992), 1-43.
- [KKS] N. Korevaar, R. Kusner, and B. Solomon, The Structure of Complete Embedded Surfaces with Constant Mean Curvature, *J. Differential Geom.* 30 (1989), 465-503.
- [LR] G. Levitt, H. Rosenberg. Symmetry of constant mean curvature hypersurfaces in hyperbolic space, *Duke Math. Journal*, vol 52, no 1 (1985).
- [O] R. Osserman. A Survey of Minimal Surfaces, Dover Publications, New York (1969).
- [P] K. Polthier. New periodic minimal surfaces in \mathbb{H}^3 . Proceedings of the Centre for Mathematics and its Applications. Australian National University. Edited by G. Dzuik, G. Huisken, and J. Hutchinson. vol. 26 (1991).
- [RUY] W. Rossman, M. Umehara, and K. Yamada. Irreducible CMC-c surfaces in $\mathbb{H}^3(-c^2)$ with positive genus. preprint.
- [S] R. Schoen. Uniqueness, Symmetry, and Embeddedness of Minimal Surfaces. *J. Differential Geom.*, 18 (1983), 791-809.
- [UY1] M. Umehara, and K. Yamada. Complete Surfaces of Constant Mean Curvature One in the Hyperbolic 3-Space. *Ann. of Math.*, 137 (1993), 611-638.
- [UY2] M. Umehara, K. Yamada. A Parametrization of the Weierstrass Formulae and Perturbation of Some Complete Minimal Surfaces of \mathbb{R}^3 into the Hyperbolic 3-Space. *J. Reine Angew. Math.*, 432 (1992), p93-116.

- [UY3] M. Umehara, K. Yamada. Surfaces of Constant Mean Curvature c in $\mathbb{H}^3(-c^2)$ with Prescribed Hyperbolic Gauss Map. *Math. Ann.*, 304 (1996), 203-224.
- [UY4] M. Umehara, and K. Yamada. A Duality on CMC Surfaces in Hyperbolic Space, and a Hyperbolic Analogue of the Osserman Inequality. To appear in *Tsukuba J. Math.*.

